

HIGHLIGHT

[View Article Online](#)
[View Journal](#) | [View Issue](#)

Research highlights

Cite this: *Lab Chip*, 2013, **13**, 3609

DOI: 10.1039/c3lc90079g

www.rsc.org/locImee G. Arcibal,^a Justin R. Smith,^a Mehmet R. Dokmeci^{b,c} and Ali Khademhosseini^{*b,d,e}

Anti-thrombus coating for on-going blood assays

While microfluidic platforms have widespread applicability for medical assays, their advantages have yet to be exploited for whole blood assays due to the limited hemocompatibility of the materials used to fabricate the devices. Common materials such as polydimethylsiloxane (PDMS), polycarbonate, silicon, and glass cause both blood proteins and platelets to accumulate quickly at the device surface, which triggers the blood clotting cascade and the formation of thrombi. These thrombi, in turn, occlude the channels of the device, increasing back pressure and rendering it inoperable after a short time. Consequently, long-term studies of whole blood mixtures for separation, bioanalysis and diagnostics of different proteins, co-factors, or potential pathogens cannot be completed. To circumvent these issues, researchers have previously examined the use of radiation and various polymeric coatings to create more hemocompatible materials.^{1,2} These treatments have improved the hemocompatibility of the devices by reducing protein and cell adhesion as well as increasing wettability, however, they have yet to prove suitable for long-term studies.

Zhang *et al.*³ have recently reported the use of a commercially available sulfobetaine polymer as a surface modification for PDMS devices to generate a microfluidic device suitable for continuous assay use. Betaine polymers presenting phosphorylcholine, sulphite, and carboxy groups have previously been shown to resist and reduce protein adsorption in 100% plasma⁴ as well as impart hydrophilicity to the modified substrates. The sulphite moiety in particular has been shown to reduce platelet attachment, activation of immune cells in the blood and potential inhibition of the

blood clotting cascade. Employing a sulfobetaine monomer (SBMA), PDMS substrates were modified through a surface-initiated polymerization reaction to covalently bind the polymer onto the surface. Reaction conditions were controlled to yield thicknesses of 1–2 µm.

The authors first characterized the properties of the modified surfaces in terms of stability, wettability, and protein adsorption. SBMA-coated PDMS surfaces were found to endure sonication, oxidative conditions, autoclave sterilization, and aging in serum without any deviation in thickness from initial measurements, indicating the chemical and physical stability of the modification. Moreover, they determined that the surface was transformed from hydrophobic to hydrophilic. The modification protocol was found to decrease static water contact angles (20.8° versus $31\text{--}90^\circ$) compared to previous ozone grafting methods. Additionally, protein adsorption on the SBMA surfaces was found to decrease by 96% when compared to the unmodified PDMS surface after exposure to fibrinogen, a key blood clotting protein. This low adsorption implies that the modified surfaces may be able to further reduce platelet attachment and the following thrombus formation.

Subsequent studies employing continuous flows of whole bovine blood demonstrated that the SBMA coating was able to prevent the generation of large thrombi within the channels of the device even after 45 min of continuous flow of whole bovine blood (Fig. 1). Untreated devices, on the other hand, had thrombi form within 25–60 min of initial flow. Analysis of

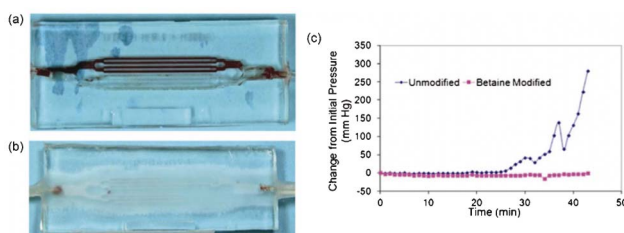


Fig. 1 Results from whole blood tests. Optical micrographs of (a) an unmodified device and (b) a betaine modified device. (c) Pressure change within both devices over time. Increase in pressure in the unmodified device is due to the formation of thrombi within the device channels. Figure adapted and reprinted with permission from the Royal Society of Chemistry from Zhang *et al.*³

^aUS Army Corps of Engineers Construction Engineering Research Laboratory, Champaign, IL 61822, USA

^bCenter for Biomedical Engineering, Department of Medicine, Brigham and Women's Hospital, Harvard Medical School, Cambridge, Massachusetts 02139, USA.

E-mail: aлик@rics.bwh.harvard.edu

^cHarvard-MIT Division of Health Sciences and Technology, Massachusetts Institute of Technology, Cambridge, Massachusetts 02139, USA

^dWyss Institute for Biologically Inspired Engineering, Harvard University, Boston, Massachusetts 02115, USA

^eWorld Premier International – Advanced Institute for Materials Research (WPI-AIMR), Tohoku University, Sendai 980-8577, Japan

Highlight

Lab on a Chip

thrombus formation determined that the modified devices resulted in an average of 5–10 fold reduction in thrombus accumulation *versus* the unmodified devices.

Zhang *et al.* have demonstrated a stable surface modification capable of not only inhibiting protein adsorption, but improving wettability and blood compatibility. Such a coating has numerous applications for devices and platforms that require continuous flow of whole blood, including dialysis-like systems capable of pathogen or toxin removal from the bloodstream or an artificial lung with high oxygen transfer rates. Moreover, SBMA coatings could also be utilized on devices implanted within the body to prevent clot formation as well as reducing the possibility of an immune response due to the decreased activation of the related cells. Lastly, coated microfluidic devices could further be used to help develop new forms of anti-coagulants and blood thinners more suitable for extended use in patients without the increased bleeding risk currently associated with heparin and warfarin.

High throughput cancer cell characterization

Cellular biomechanics plays an important role in the spread of cancer and other invasive diseases as the affected cells must undergo biochemical and cytoskeletal changes in order to travel through the bloodstream. As these cells travel, their trajectory is affected by their viscoelastic and frictional properties. Researchers have employed multiple techniques to examine these properties, including micropipette aspiration,⁵ atomic force microscopy,⁶ and microrheology.⁷ While these techniques have yielded both detailed and quantitative information, they suffer from low throughput and do not offer insight about the relative significance between the viscoelastic and frictional properties of the cells. Microfluidics has previously been tapped in attempts to create devices that can increase throughput;⁸ however, these systems have only generated semi-quantitative data.

In an effort to address these issues, Byun *et al.*⁹ have developed a suspended microchannel resonator (SMR) capable of interrogating the relationship between the viscoelastic and frictional properties of a cell by monitoring its buoyant mass and velocity. The SMR consists of a hollow microchannel embedded in a silicon cantilever with a constriction located near the apex of the resonator (Fig. 2). For each experiment, a solution which includes cells that are denser than the surrounding fluid is guided into the device. As the cell enters the SMR, the resonant frequency of the chip is lowered by an amount that depends on the buoyant mass of the cell and its position away from the resonator base. The SMR is capable of examining a few thousand cells per hour, yielding information about each cell's buoyant mass (related to cell size) as well as its entry velocity, transit velocity, and passage time through the constriction.

The authors first validated their method with a human lung carcinoma line, H1975. Cell passage time was found to relate

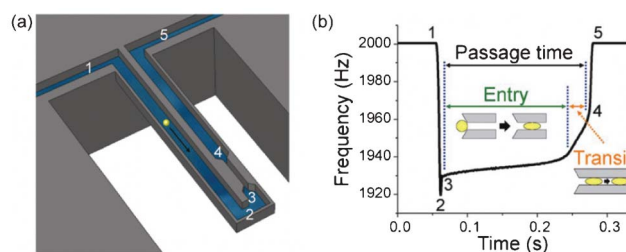


Fig. 2 Schematic diagram of the instrument and data extracted from the measurement. (a) SMR device illustrating the microchannel resonator and constriction. (b) Resonant frequency response of the SMR as a cell passes through the channel. Numbers 1–5 indicate positions shown in (a) as the cell passes through the different positions in the device. Figure adapted and reprinted with permission from Byun *et al.*⁹

to its buoyant mass through a power law relationship as expected from previous studies. However, passage times for the cells ranged four orders of magnitude when correlated to buoyant mass (1000-fold larger range *versus* previous reports). Byun *et al.* postulate that this deviation may be due to the orientation of the cells upon entering the constriction in addition to inherent biological variations. Other mammalian cell lines (including embryonic fibroblasts, variations of the mouse lung cancer line T_{Met}, human lung cancer lines, and mouse L1210) were also found to exhibit the power law dependence between passage time and buoyant mass. It was determined that cell lines with a higher propensity for travelling and invasion (metastatic potential) displayed shorter passage times when compared with those with a lower metastatic potential.

H1975 cells were also employed to examine the effects of deformability and surface friction on the passage of cells through the constriction. The cells were subjected to two different conditions, treatment with latrunculin B (LatB) to disrupt the cytoskeleton and microchannel treatment with poly-L-lysine to impart a positive charge to the surface. Cytoskeleton disruption increased cell deformability and consequently decreased passage time of the cells, while increasing entry and transit velocities. The positive lysine coating had the opposite effect on the cells compared to LatB, as the negatively charged cell surface interacted with lysine to decrease the entry and transit velocities. The information gained about deformability and friction during these studies were also found to be a unique indicator of cell state and metastatic potential where the higher entry and transit velocities point to a higher metastatic potential. This finding is not unexpected as the ease in manoeuvrability of the cells would directly correlate with their ability to invade new regions of the body.

The SMR platform developed by Byun *et al.* provides high throughput data with high spatial precision that has previously been lacking in the study of cellular biomechanics, particularly the viscoelastic and frictional properties associated with invasive diseases such as cancer. The information gained from these studies as well as from further use of this

device will yield fundamental knowledge about how these diseases spread and what factors mitigate the speed of the spread. Further, this platform can be used as a diagnostic tool to examine blood for elusive circulating tumour cells in efforts to diagnose and begin treatment at an early stage of the disease.

Enhancing engineered tissue integration

At present, other than the scarce supply of donor organs, there is a lack of feasible approaches to regenerate or replace damaged tissues and organs within the human body. Tissue engineering provides a unique opportunity to address this problem by constructing viable replacements for implantation in an *in vitro* setting. While there has been success in replacing avascular tissue, many of the other tissue constructs require the creation and integration of blood vessels with the existing organs for proper function. Recent research has shown that to achieve this type of vascularization, cells that have formed vascular networks exogenously should be grafted in conjunction with the replacement tissue to improve survival.^{10,11} However, these approaches have been hampered by a lack of pre-organized structure for these cells to form vasculature as it relies on the cells themselves to spontaneously self-assemble, which has yielded limited success.

Baranski *et al.*¹² have recently employed a patterned microtissue mold to organize and construct aligned endothelial cell cords capable of generating new capillaries along the entire cord (Fig. 3). These cell cords consisted of a collagen core surrounded by both human and mouse endothelial cells (ECs) patterned within a PDMS mold where the cells self-assembled into cords. The cords were subsequently implanted in mice with host blood beginning to perfuse through the cord within days and mature capillaries forming within weeks. The patterned cords were found to exhibit better function and survival than randomly organized endothelial networks.

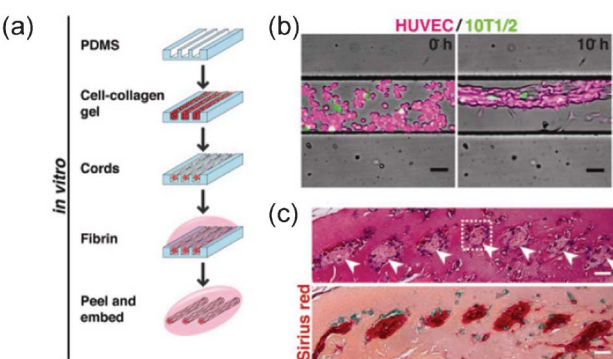


Fig. 3 Generation of EC cords. (a) Schematic representation of PDMS molding process to generate the cords. (b) Merged phase and fluorescence images of cord formation at 0 and 10 h with HUVEC cells stained with calcein AM orange and 10T1/2 cells stained with calcein AM green. (c) Histological staining of paraffin-embedded cord-containing tissue constructs. Figure adapted and reprinted with permission from Baranski *et al.*¹²

Moreover, the authors demonstrated that the human EC cords integrated well with the host mouse cells where both cell types contributed to the growth of capillaries. These results offer a template for engineering vascular architecture to exert function upon engineered tissue. This patterned approach allows for the rapid vascularization of endothelial cell cords into host tissue, creating the necessary next step to engineering complex tissues (*e.g.*, kidney and liver) to provide the geometric spacing and alignment needed for metabolic function.

The authors then observed the growth of the EC cords into capillaries over the course of 28 days. By five days after implantation, different blood vessels began to normalize in diameter, while by 14 days mature capillaries had formed. At 28 days, contractile pericyte cells became tightly associated with the capillaries, which was essential for properly regulating blood flow within capillaries. When the authors verified that the cords were perfused with host blood, they also found that the microvascular network was chimeric in composition, containing both host and implanted cells in some vessels. This finding demonstrates the rapid formation of the connections between the implanted cords and the host tissue. After demonstrating that the patterned EC cords not only survived following implantation, but also formed capillaries and integrated to the host tissue, Baranski *et al.* examined whether the cords improved tissue function by implanting primary hepatocytes in mice. By comparing hepatocyte aggregates containing EC cords with aggregates randomly seeded with ECs and with aggregates without any cords, the authors showed that the aggregates having EC cords displayed significantly higher levels of albumin activity. This increase indicates better integration of these implants with the existing tissue due to the cords, creating direct access to the blood-carrying vasculature of the host mouse, which enhanced cell function.

In this study, the authors demonstrated that EC growth can be controlled by the use of geometric patterning for directed prevascularization of tissues. The patterning control offered here improved the perfusion of cells inside the implanted constructs, presenting a way to improve the tissue integration process by enhancing blood supply. Further, the prevascularization improved the speed and the extent of vascularization response through a combination of both angiogenesis and vasculogenesis. This directed prevascularization was also found to enhance the function and the survival of the implanted hepatic tissue. In the future, this method can be used to yield fundamental information about the effects of vascular networks on tissue oxygenation and function and could potentially lead to the design of custom vascular architectures.

References

1. J. Zhou, A. V. Ellis and N. H. Voelcker, *Electrophoresis*, 2010, **31**, 2–16.
2. M. Ebara, J. M. Hoffman, P. S. Stayton and A. S. Hoffman, *Radiat. Phys. Chem.*, 2007, **76**, 1409–1413.

- 3 Z. Zhang, J. Borenstein, L. Guiney, R. Miller, S. Sukavaneshvar and C. Loose, *Lab Chip*, 2013, **13**, 1963–1968.
- 4 Z. Zhang, T. Chao, S. Chen and S. Jiang, *Langmuir*, 2006, **22**, 10072–10077.
- 5 R. M. Hochmuth, *J. Biomech.*, 2000, **33**, 15–22.
- 6 S. Yamada, D. Wirtz and S. C. Kuo, *Biophys. J.*, 2000, **78**, 1736–1747.
- 7 A. Adamo, A. Sharei, L. Adamo, B.-K. Lee, S. Mao and K. F. Jensen, *Anal. Chem.*, 2012, **84**, 6438–6443.
- 8 S. C. Hur, N. K. Henderson-MacLennan, E. R. B. McCabe and D. Di Carlo, *Lab Chip*, 2011, **11**, 912–920.
- 9 S. Byun, S. Son, D. Amodei, N. Cermak, J. Shaw, J. H. Kang, V. C. Hecht, M. M. Winslow, T. Jacks, P. Mallick and S. R. Manalis, *Proc. Natl. Acad. Sci. U. S. A.*, 2013, **110**, 7580–7585.
- 10 K. Kaufman-Francis, J. Koffler, N. Weinberg, Y. Dor and S. Levenberg, *PLoS One*, 2012, **7**, e40741.
- 11 J. Koffler, K. Kaufman-Francis, S. Yulia, E. Dana, A. P. Daria, A. Landesberg and S. Levenberg, *Proc. Natl. Acad. Sci. U. S. A.*, 2011, **108**, 14789–14794.
- 12 J. D. Baranski, R. R. Chaturvedi, K. R. Stevens, J. Eyckmans, B. Carvalho, R. D. Solorzano, M. T. Yang, J. S. Miller, S. N. Bhatia and C. S. Chen, *Proc. Natl. Acad. Sci. U. S. A.*, 2013, **110**, 7586–7591.